GEOSCIENCE FRONTIERS 2(2) (2011) 125–135

available at www.sciencedirect.com

China University of Geosciences (Beijing)

GEOSCIENCE FRONTIERS

journal homepage: www.elsevier.com/locate/gsf

ORIGINAL ARTICLE

The influence of temperature, pressure, salinity and capillary force on the formation of methane hydrate

Zhenhao Duan [a,*], Ding Li [a], Yali Chen [b], Rui Sun [c]

[a] *Key Laboratory of the Earth's Deep Interior, Institute of Geology and Geophysics, Chinese Academy of Sciences, Beijing 100029, China*
[b] *School of Earth Sciences and Resources, China University of Geosciences, Beijing 100083, China*
[c] *Northwest University, Xi'an 710069, China*

Received 16 November 2010; accepted 1 March 2011
Available online 3 April 2011

KEYWORDS
Methane hydrate;
ab initio potential;
Salinity;
Porous sediment;
Forming conditions;
Phase equilibria

Abstract We present here a thermodynamic model for predicting multi-phase equilibrium of methane hydrate liquid and vapor phases under conditions of different temperature, pressure, salinity and pore sizes. The model is based on the 1959 van der Waals–Platteeuw model, angle-dependent *ab initio* intermolecular potentials, the DMW-92 equation of state and Pitzer theory. Comparison with all available experimental data shows that this model can accurately predict the effects of temperature, pressure, salinity and capillary radius on the formation and dissociation of methane hydrate. Online calculations of the $p-T$ conditions for the formation of methane hydrate at given salinities and pore sizes of sediments are available on: www.geochem-model.org/models.htm.

1. Introduction

Gas hydrate (or clathrate hydrate) is composed of cages bonded by water molecules and guest molecules encapsulated in the cages through van der Waals forces between the guest and water molecules. Only when the cage space and the size of guest molecules match each other can a stable clathrate hydrate be formed. At present, gas hydrate is discovered in oil and gas pipelines, marine sediments, permafrost (Sloan, 1998), comets and some foreign planets (Lunine and Stevenson, 1987). Presently known natural gas reserve stored in gas hydrate (mainly methane hydrate) is considered to be huge. 1 m^3 of methane hydrate can release 164 m^3 of methane gas. Thus, methane hydrate is considered to be highly compressed natural gas and an obvious potential clean energy source and a substitute for fossil fuels. In addition, release of methane gas from oceanic and permafrost hydrates into the atmosphere could have an important impact on global warming

* Corresponding author.
E-mail address: duanzhenhao@yahoo.com (Z. Duan).

Peer-review under responsibility of China University of Geosciences (Beijing).
doi:10.1016/j.gsf.2011.03.009

Production and hosting by Elsevier

(Dickens, 2003). Xu and Germanovich (2006) have proposed that gas hydrate melting can trigger submarine landslides.

Methane hydrate under high pressure and low temperature is stable. Fig. 1 is the phase diagram of the CH_4–H_2O binary system. Q is the quadruple invariant point, where methane hydrate (H), ice (I), water-rich liquids (L) and CH_4-rich gas (V) coexist. Line AQB shows p–T conditions when H–I–V and H–L–V reach equilibrium and it also indicates the boundary on which methane hydrate is stable. Based on phase equilibrium conditions, the region on both sides of the line AQB is the two-phase region, where in the region above AQB methane hydrate is stable and below AQB methane-rich gas and liquid water or ice coexist.

Since van der Waals and Platteeuw (1959), a number of scholars have proposed thermodynamic models to calculate the equilibrium of gas hydrate. However, previous work is mostly on the gas hydrate three-phase equilibrium of bulk systems, including Parrish and Prausnitz (1972), Ng and Robinson (1976), Englezos and Bishnoi (1988), Tohidi et al. (1995), Chen and Guo (1998), Ballard and Sloan (2002), and Lee and Holder (2002). Clennell et al. (1999) and Henry et al. (1999) designed a thermodynamic model to predict the three-phase equilibrium of methane hydrate in marine sediments by using the Gibbs–Thomas equation calculating the capillary effect caused by small pores. Later, Klauda and Sandler (2001) proposed a model predicting the distribution of methane hydrate in marine sediments, but parameters in these models are not accurate enough (Llamedo et al., 2004). These models overestimate the inhibitory effect of capillary force on the H–L–V equilibrium.

Most published models predict the conditions of methane hydrate formation using the Kihara potential model, where parameters are derived from the experimental data of hydrate phase equilibrium and cage occupancy. While these models after assignment fit very well with experimental data, their predictive power is poor. For instance, models by Parrish and Prausnitz (1972) and the CSMHYD model by Sloan (1998) predicting the hydrate phase equilibrium only apply when pressure is lower than (400–500) $\times$ 10^5 Pa. In addition, the Kihara potential energy surface obtained by the experimental data doesn't agree with that of Tee et al. (1966) whose calculations used the second virial coefficient and viscosity data. Hence, the Kihara potential model cannot accurately describe the interactions between water molecules and guest molecules. Potential parameters obtained simply by fitting macroscopic system experimental data cannot accurately reflect the potentials of microscopic molecular interactions. Therefore, in this study we use the atomic site–site potentials model. This model takes into account the molecular interaction's dependence on the angle, and its parameters are calculated using the *ab initio* method instead of being derived from macroscopic experimental data.

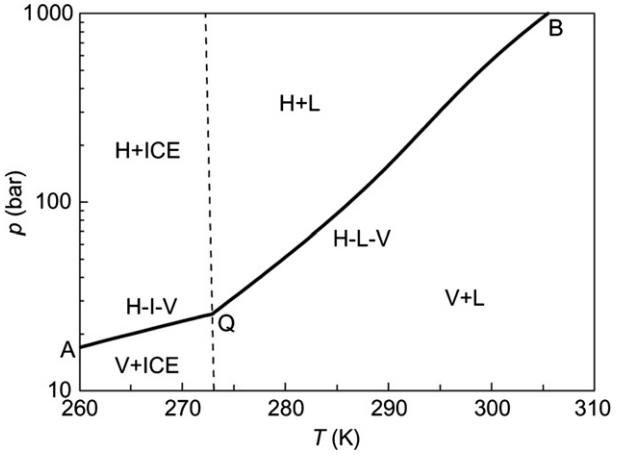

Figure 1 p–T phase diagram of the CH_4–H_2O binary system at low temperatures.

The goal of this study is to build an accurate H–L–V three-phase equilibrium model to predict the effect of temperature, pressure, salinity and capillary force on the formation and dissociation of methane hydrate based on the van der Waals and Platteeuw (1959) model, *ab initio* intermolecular potentials, equation of state by Duan et al. (1992b) and Pitzer (1991) theory. Among the models, the basic hydrate model by van der Waals and Platteeuw (1959) is used to describe the chemical potential of the hydrate phase; the *ab initio* intermolecular potentials is used to calculate the Langmuir constant; and Duan et al.'s (1992b) equation of state is applied to calculate the fugacity of methane gas.

2. Thermodynamic model of hydrate

2.1. Methane hydrate formation temperature and pressure in pure water

When the methane hydrate phase is in equilibrium with the liquid water or ice phase, the chemical potentials of water in the former (μ_w^H) and in the later (μ_w^L) are the same, namely

$$\mu_w^H = \mu_w^L \tag{1}$$

If we make the chemical potential of empty hydrate lattice a reference state at the same temperature and pressure, then

$$\Delta\mu_w^H = \mu_w^\beta - \mu_w^H = \mu_w^\beta - \mu_w^L = \Delta\mu_w^L \tag{2}$$

Therefore, theoretical models that predict formation conditions of gas hydrate consist of two parts: one for gas hydrate phase and the other for pure water phase (liquid water or ice). The former is usually based on van der Waals and Platteeuw (1959) adsorption isotherm theory and the latter is based on Holder et al.'s (1980) expressions.

Based on classical statistic mechanics and Langmuir adsorption isotherm theory, van der Waals and Platteeuw (1959) derived the expression for the difference of chemical potentials between empty hydrate phase and filled hydrate phase:

$$\Delta\mu_w^H(T,p) = -RT\sum_{i=1}^{2} v_i \ln\left(1 - \sum_{j=1}^{N_C}\theta_{ij}\right) \tag{3}$$

where v_i is the number of i-type cages per water molecule (in sI-type hydrate, $v_i = 1/23$ for small cages and $v_i = 3/23$ for big cages); N_C is the number of components that can form hydrate; θ_{ij} is the fractional occupancy of small cavities with j-type guest molecules whose expression is:

$$\theta_{ij} = \frac{C_{ij}f_j}{1 + \sum_{j=1}^{N_C} C_{ij}f_j} \tag{4}$$

where f_j is the fugacity of guest molecules in each phase; C_{ij} is the Langmuir constant of guest molecule j in i-type cages, which is usually calculated by intermolecular potential functions. The definition of C_{ij} is:

$$C_{ij}=\frac{1}{RT}\int\int \exp\left[-\frac{W(r,\Omega)}{kT}\right]\mathrm{d}r\mathrm{d}\Omega \quad (5)$$

where r and Ω represent position vector and orientation vector of the guest molecule in the cavity, respectively; $W(r,\Omega)$ is the interaction potential between the guest molecule and water molecules surrounding it.

According to the above analysis, the key to predict the equilibrium conditions of methane hydrate is to calculate the Langmuir constants with accurate intermolecular potentials. The constants are related to temperature and reflect the interaction between gas and water molecules in cavities of hydrate lattice. However, most previous models obtain the Langmuir constant based on the Kihara potential model, whose parameters are regressed from experimental data of hydrate equilibrium. In the last two decades, the *ab initio* potentials of CH_4–H_2O system have been studied by Bolis et al. (1983), Latajka and Scheiner (1987), Novoa et al. (1991), Szczesniak et al. (1993) as well as Cao et al. (2001) and Klauda and Sandler (2002), but the results differ among different research groups.

After careful examination of their studies, we adopted the results of Szczesniak et al. (1993), because: (1) they used larger basis sets and employed more accurate QM calculations: the *ab initio* potential energy surfaces were calculated at MP2 level and corrected at MP4 level; (2) the basis set superposition error (BSSE) of interaction energies was included, which was neglected by many studies in the twentieth century, hence the results are supposed to be more accurate; and (3) more types of orientation were included than other studies. Although Cao et al. (2001) chose more basis sets and calculated the *ab initio* potentials of many CH_4–H_2O configurations, they had less types of orientation between CH_4 and H_2O than Szczesniak et al. (1993). We believe that enough orientation types are essential in describing the angle-dependency of intermolecular potential surfaces. In addition, Szczesniak et al.'s (1993) results are better than Klauda and Sandler's (2002) in QM calculation level and number of basis sets. Therefore, we chose *ab initio* potentials determined by Szczesniak et al. (1993) in this study.

If we derive the Langmuir constants directly from Equation (5), the results should confirm to an empiric formula. We found that Coulombic charge–charge interaction plays an important role in the interaction potentials of gas and water molecules, so we include an electrostatic term in the formula. At first, we tried to fit the *ab initio* potential with a spherical Lennard–Jones 12-6 or Kihara potential model, but these models cannot represent the *ab initio* potential surface adequately. Therefore, we chose the atomic site–site potential model, where the interaction sites are located on every atom in the CH_4 and H_2O molecules. For water molecules, the interaction site that is located on the bisector of H–O–H angle is also included. So the combined form of the Lennard–Jones Formula and Coulumb Law is used to fit the *ab initio* potential, which has the following form:

$$E(r_{ij})=\sum_i\sum_j\left\{4\epsilon_{ij}\left[\left(\frac{\sigma_{ij}}{r_{ij}}\right)^{12}-\left(\frac{\sigma_{ij}}{r_{ij}}\right)^{6}\right]+\frac{q_iq_j}{r_{ij}}\right\} \quad (6)$$

where i, j summation run over all C and H centers in methane molecules and O, H, M centers in water molecules, respectively.

We use a nonlinear least square method to fit *ab initio* data from Szczesniak et al. (1993) to fit the CH_4–H_2O system, and Boltzmann's constant to weight the target function to make the difference between results of *ab initio* calculation and the prediction of formula (6) small. The target function is the same as

Table 1 Atomic site–site Lennard-Jones potential parameters for the CH_4–H_2O system.

CH_4	H_2O	ϵ/k (K)	σ (Å)
C	O	61.40	3.627
C	H	22.4	2.2
C	M	0.0	0.0
H	O	40.79	2.777
H	H	15.1	1.5
H	M	0.0	0.0

Klauda and Sandler (2002) and Anderson et al. (2004). The parameters in formula (6) are calculated at MP2 level and corrected at MP4 level. Experimental geometric parameters of CH_4 are: r(CH) = 1.09 Å and angle between H–C–H is 109. 4722°. The TIP4P model (Jorgensen et al., 1983) is used to describe the geometric structure of water: r(OH) = 0.9572 Å; angle between H–O–H is 109. 4722°. Another interaction site "M" located at the bisector of H–O–H is 0.15 Å away from the oxygen atom and on the hydrogen atoms' side. The electrostatic formula in TIP4P can result in better fitting, so we choose $q_O = 0.0$, $q_H = 0.52$, $q_M = -1.04$. In the CH_4–H_2O system, we use other parameters including ϵ, σ, etc., and the charge of C and H atoms in some CH_4 molecules to do nonlinear fitting of the *ab initio* potential data. These parameters are listed in Tables 1 and 2. In addition, the atom site–site model used in this study can represent the results of Szczesniak et al. (1993) adequately according to Fig. 2.

Another important point in our model is to calculate fugacities of gas components with precise thermodynamic model. In H–L–V equilibrium, fugacities of methane in hydrate, liquid and gas are the same, namely:

$$f^{H}_{CH_4}=f^{L}_{CH_4}=f^{V}_{CH_4} \quad (7)$$

There are, at present, many equations of state predicting thermodynamic properties of pure gas or gas mixtures. In this study, we use the equation of state of Duan et al. (1992b) to calculate fugacities of methane in gas. While many equations of state are capable of calculating fugacity in pure methane system, the DMW-92 equation of state is the most precise in predicting p–V–T properties of methane under high pressure (larger than 100 MPa). Fig. 3 is a comparison of Setzmann and Wagner's (1991) equation of state with those of C–P (Chueh and Prausnitz, 1967), S–RK (Soave, 1972), P–R (Peng and Robinson, 1976), and DMW-92 (Duan et al., 1992b) on their predictions of methane molar volume along the methane hydrate stable curve under temperatures larger than 270 K. Since Setzmann and Wagner's equation of state can represent the molar volume of the methane in a wide range of temperatures and pressures with an uncertainty less than 0.1%, the equation

Table 2 Partial charges of CH_4 and H_2O molecule.

Atom	q
C_{CH_4}	−0.48
H_{CH_4}	0.12
O_{H_2O}	0.00
H_{H_2O}	0.52
M_{H_2O}	−1.04

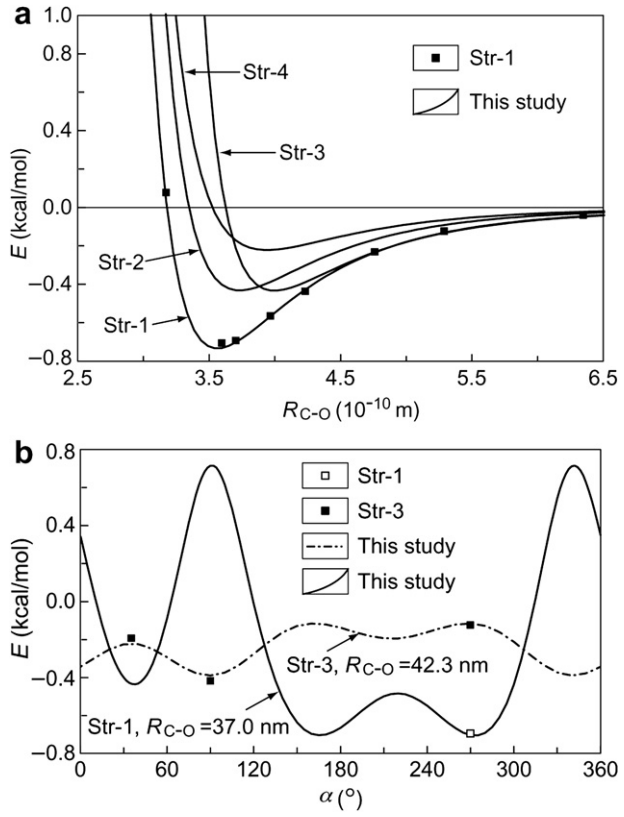

Figure 2 The angle dependence of the potential energy surface of CH_4–H_2O: (a) The variation of the intermolecular potential with distance and (b) the variation of the intermolecular potential with angle alpha (angle between the bond C–H1 and *z*-axis in *yz*-plane). Solid squares and open squares represent the *ab initio* data obtained by Szczesniak et al. (1993) at MP2 level; solid lines and dotted line are the atomic site–site potential energy predicted for different orientations.

becomes standard to testing the accuracy of the above equations. From Fig. 3, we can conclude that DMW-92 (Duan et al., 1992b) equation of state is the most precise under high pressure with an average error less than 1%. Because the goal of this study is to

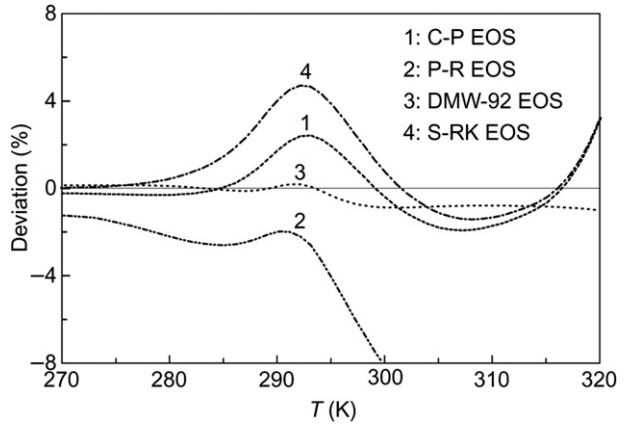

Figure 3 The average deviation of different equations of state from the equation Setzmann and Wagner (1991). The source of experimental data: 1. Chueh and Prausnitz (1967); 2. Peng and Robinson (1976); 3. Lunine and Stevenson (1987); 4. Soave (1972).

predict the equilibrium of methane hydrate under low temperature and high pressure, the DWM-92 (Duan et al., 1992b) equation of state is used to calculate the fugacity of methane.

According to Holder et al. (1980), the difference of chemical potentials between empty hydrate and water or ice is:

$$\frac{\Delta\mu_w^L(T,p)}{RT}=\frac{\Delta\mu_w^0(T_0,0)}{RT_0}-\int_{T_0}^{T}\left(\frac{\Delta h_w^{\beta-L}}{RT^2}\right)dT+\int_0^p\left(\frac{\Delta V_w^{\beta-L}}{RT}\right)dp-\ln a_w \tag{8}$$

where $\Delta\mu_w^0(T_0,0)$ is the difference of chemical potentials between empty hydrate and ice when $T = 273.15$ K, $p = 0$ Pa; $\Delta h_w^{\beta-L}$ and $\Delta V_w^{\beta-L}$ is the difference of molar enthalpy and the difference of molar volume, respectively, between empty hydrate lattice and liquid water; a_w is the activity of water.

Δh_w^{π}, the enthalpy change, is:

$$\Delta h_w^{\pi}=\Delta h_w^0(T_0)+\int_{T_0}^{T}\Delta C_p^{\pi}dT \tag{9}$$

ΔC_p^{π}, the difference of heat capacity between empty hydrate and water or ice, is:

$$\Delta C_p^{\pi}=\Delta C_p^0(T_0)+b(T-T_0) \tag{10}$$

In formulas (9) and (10), Δh_w^0 and ΔC_p^0 are the differences of molar enthalpy and molar heat capacity, respectively, between empty hydrate lattice and ice, where b is the temperature coefficient of heat capacity. The values of Δh_w^0 and ΔC_p^0 come from the experimental data of methane hydrate three-phase equilibrium in a CH_4–H_2O system (Sun and Duan, 2005); the value of ΔC_p is taken from Parrish and Prausnitz (1972). Table 3 shows the values of$\Delta\mu_w^0$, Δh_w^0 and ΔC_p^0 for sI hydrate. The molar volume of liquid water, V_w^{β}, can be calculated from Sun et al.'s (2003) equation of state, which is given as the following formula:

$$V_w^{\beta}(T,p)=\left(11.820+2.217\times10^{-5}T+2.242\times10^{-6}T^2\right)\frac{10^{-30}N_A}{N_w^{\beta}}\times\exp\left[-3.5\times10^{-4}(p-0.1)+7.07\times10^{-6}(p-0.1)^{1.5}\right] \tag{11}$$

where N_A is the Avogadro constant and N_w^{β} is the number of water molecules in every hydrate crystal. For sI hydrate, $N_w^{\beta}=46$. The unit of pressure and temperature is MPa and K, respectively.

To calculate the pressure of H–L–V equilibrium under a given temperature, we assume that the initial value of pressure is p_1 and then C_{ij}, $f_{CH_4}^V$, $\Delta h_w^{\beta-L}$, $\Delta V_w^{\beta-L}$ and a_w are calculated. The above values are substituted in Equations (3) and (8) to calculate $\Delta\mu_w^H$ and $\Delta\mu_w^L$. Finally we compare $\Delta\mu_w^H$ and $\Delta\mu_w^L$. If the difference between them is small enough (e.g. 1×10^{-2}), p_1 is the equilibrium pressure when the temperature is T; otherwise, we change the value of p_1 and repeat until the suitable pressure is found. In the

Table 3 Thermodynamic reference properties for sI-type hydrate ($T_0 = 273.15$ K).

$\Delta\mu_w^0$ (J/mol)	1202
Δh_w^0 (J/mol)	1300
$\Delta h_w^{\alpha-L}$ (J/mol)	−6009.5
$\Delta C_p^{\beta-L}$ (J/(mol·K))	$-38.12 + 0.141\times(T - T_0)$
$\Delta C_p^{\beta-\alpha}$ (J/(mol·K))	$0.565 + 0.002\times(T - T_0)$

course of above calculations, the Newton iteration method or bisection method is used. When the difference between $\Delta\mu_w^H$ and $\Delta\mu_w^L$ is smaller than 1×10^{-2}, we usually think of the assumed pressure as the equilibrium pressure with an error less than 0.1% (Fig. 4). According to Fig. 4, the prediction accuracy of this model is better than that of the CSMHYD model, whose parameters are from the regression of experimental data.

2.2. Influence of electrolyte

While an electrolyte cannot change the chemical potential of water in the hydrate phase because it cannot get into the hydrate lattice of, it does influence the H–L–V equilibrium of methane hydrate by changing the activity of water and methane in solutions. Zatsepina and Buffett (1998) calculated the activity coefficients of water and methane in solutions with the Aasberg-Peterson model (1991). However, the Aasberg-Peterson model underestimates the influence of salting-out effect on methane solubility under gas–liquid equilibrium (e.g. underestimating methane activity coefficient in electrolyte solutions), and overestimates the activity coefficient of water under low temperature ($T < 303$ K). The reason of the inaccuracy of the above model is that its parameters of water–salt and gas–salt reactions come from high temperature experimental data (the pressure of gas phase of the salt solution is obtained under 373 K, and the solubility of gas is obtained under 323 K). According to experimental data, the activity coefficient of dissolved methane, γ_{CH_4}, decreases as the temperature increases from 273 K to 373 K. For instance, the γ_{CH_4} of 1 mol solution of NaCl is 1.40 under 273 K and is 1.26 under 323 K. The methane solubility model of Duan et al. (1992a) used by Clennell et al. (1999) and Henry et al. (1999) underestimates the activity coefficient of methane in electrolyte solutions under temperatures less than 303 K, but Duan and Mao (2006) have corrected this error recently.

We use the Pitzer (1991) model to calculate the activity coefficient of water and predict the temperature and pressure of H–L–V equilibrium in different electrolyte solutions (Duan and Sun, 2006). The parameters in this model are different as the temperature changes, and we use this method to calculate the a_w of seawater in this study.

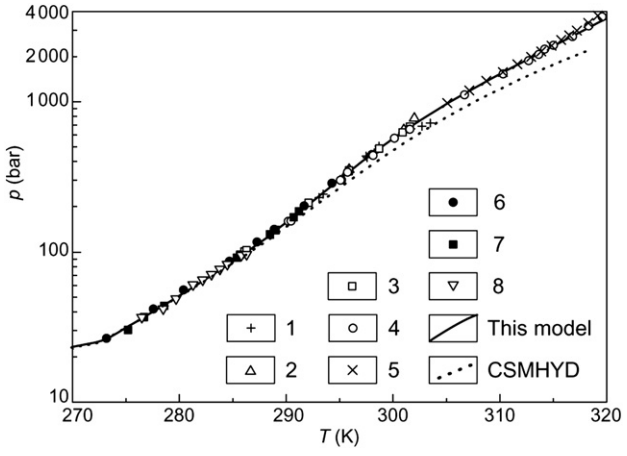

Figure 4 Prediction of equilibrium pressure of CH_4 hydrate in the CH_4–H_2O system. The source of experimental data: 1. Jager and Sloan (2001); 2. Kobayashi and Katz (1949); 3. McLeod and Campbell (1961); 4. Marshall et al. (1964); 5. Nakano et al. (1999); 6. Jhaveri and Robinson (1965); 7. Verma (1974); 8. Yang et al. (2001). CSMHYD after Sloan (1998).

This paper omits the formula to calculate a_w based on the Pitzer model for convenience. The following is the equation of the relationship between a_w and ϕ, the osmotic coefficient:

$$\ln a_w = -\frac{M_w}{1000}\left(\sum_i m_i\right)\phi \tag{12}$$

where M_w is molecular weight of water and m is the amount of substance of solute particle; i represents the sum of all solutes (including cations, anions and uncharged particles). The equation about ϕ proposed by Pitzer and Silvester (1976) and modified by Harvie et al. (1984) and Felmy and Weare (1986) is:

$$\begin{aligned}\left(\sum_i m_i\right)(\phi-1) = &-\frac{2A^\phi I^{1.5}}{1+1.2I^{0.5}} + \sum_c\sum_a m_c m_a\left(B^\phi_{ca} + ZC_{ca}\right)\\ &+ 2\sum\sum_{c<c'} m_c m_{c'}\left(\Phi^\phi_{cc'} + \sum_a m_a\varphi_{cc'a}\right)\\ &+ 2\sum\sum_{a<a'} m_a m_{a'}\left(\Phi^\phi_{aa'} + \sum_c m_a\varphi_{aa'c}\right)\\ &+ 2\sum_n\sum_c m_n m_c\lambda_{nc} + 2\sum_n\sum_a m_n m_a\lambda_{na}\\ &+ 2\sum_n\sum_c\sum_a m_n m_c m_a\zeta_{nca}\end{aligned} \tag{13}$$

where I is the ionic strength; Z is the sum of the product of amount of substance and charges of particles, namely $Z = \sum m_i|z_i|$; the subscripts c, a, and n refer to cations, anions, and uncharged particles. The summation index c represents the sum of all cations; the double summation index $c < c'$ represents the sum of all recognizable distinct cations. The same apply to anions. A^ϕ is one-third of the Debye-Huckel limiting slope and is 0.39 at 25 °C. The values of B, Φ and λ represent measurable combinations of the second virial coefficients. The values of C and ψ represent measurable combinations of the third virial coefficients.

Pitzer thought that the virial coefficients B_{cn} and ϕ_{ijk} are the function of ionic strength; C_{ca} and ψ_{ijk} have nothing to do with ionic strength. Pitzer and Mayorga (1973, 1974), Pitzer and Kim (1974), and Pitzer (1975) calculate most of the electrolyte parameters at 25 °C (e.g. the interaction parameters of water and electrolyte, including values of B, C, ϕ, and ψ). The hydrate model by Englezos and Bishnoi (1988) and Dubessy et al. (1992) is used to predict the equilibrium of hydrate in electrolyte solutions. This model is based on Pitzer–Mayorga model, whose electrolyte parameters are calculated at 25 °C. In activity coefficient models of Chen and Evans (1986), Zuo and Guo (1991), and Aasberg-Petersen et al. (1991) also calculate the electrolyte parameters at 25 °C or higher. However, we cannot overlook the dependency of activity coefficients on temperature in water–salt systems. Then the parameters at 25 °C cannot predict the permeability and activity coefficients at other temperatures. Electrolyte parameters of the studies of Na–K–Ca–Cl–SO_4–H_2O by Pabalan and Pitzer (1987), Moller (1988), and Greenberg and Moller (1989) are between 0 and 25 °C, or even higher. However, the parameters of Spencer et al. (1990) range from −55 to 25 °C. We chose their parameter values because the equilibrium of gas hydrate in electrolyte solutions is at relatively low temperatures.

In certain temperatures, we should consider the influence of pressures on activity coefficients in theoretical calculations. However, Monnin (1990) proposed that the influence is quite small and can be ignored. Based on the studies of Pitzer et al.

(1984), the parameters depend on pressure and temperature in NaCl solutions is in accordance with Monnin's (1990) conclusion. Therefore, we ignore the influence of pressures on activity coefficients of water.

The second virial coefficient λ_{ni} and the third virial coefficient ξ_{nij} represent the interaction of ions and neutrals. λ_{CH_4-i} and ξ_{CH_4-ij} have been calculated by the gas solubility model of Duan et al. (1992a) and Duan and Sun (2003) who evaluated λ_{CH_4-Na} and $\lambda_{CH_4-Na-Cl}$ based on the solubility of CH_4 in NaCl solutions. λ_{CH_4-K} is approximately equal to λ_{CH_4-Na}; and λ_{CH_4-Ca} is about twice the value of λ_{CH_4-Na}. Assume that all ξ_{CH_4-ij} is equal to $\xi_{CH_4-Na-Cl}$, λ_{CH_4-Na} is a function of pressure and temperature, and $\xi_{CH_4-Na-Cl}$ is the constant with the value of $-6.2394380 \times 10^{-3}$. Following is the formula:

$$\lambda_{CH_4-Na} = 0.099223079 + 2.5790681 \times 10^{-5} T + 0.018345140 p/T - 8.0719672 \times 10^{-6} p^2/T \quad (14)$$

All parameters of the above formula have been obtained from previous studies and it is not necessary to fit the gas–hydrate equilibrium data in solutions with corrected parameters. Figs. 5–7 compare the experimental data and the model. Though this model does not fit experimental data, we can tell from the figure that it represents the experimental results precisely.

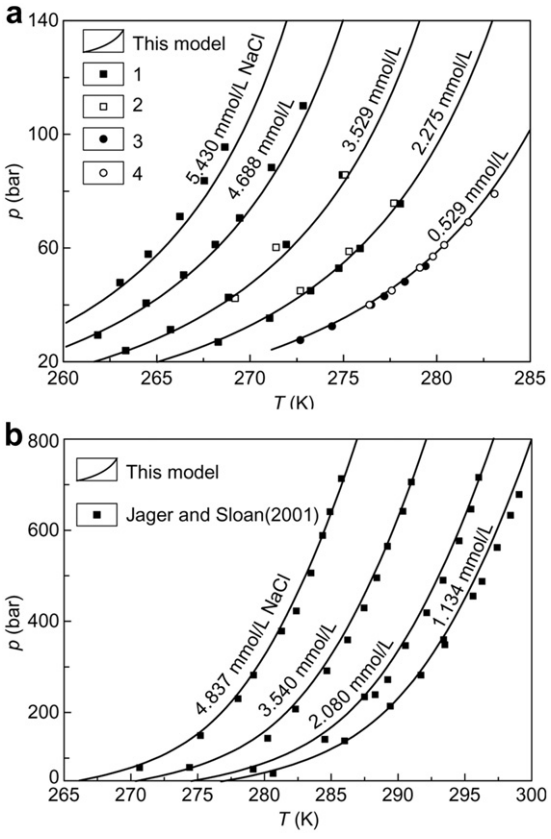

Figure 5 Prediction of the thermodynamic stability of CH_4 hydrate in CH_4–H_2O–NaCl system. (a) At pressures below 100 bar. The sources of the experimental data are: 1. De Roo et al. (1983); 2. Kharrat and Dalmazzone (2003); 3. Dholabhai et al. (1991); 4. Maekawa (2001). (b) At pressures greater than 100 bar. The source of the experimental data is: Jager and Sloan (2001).

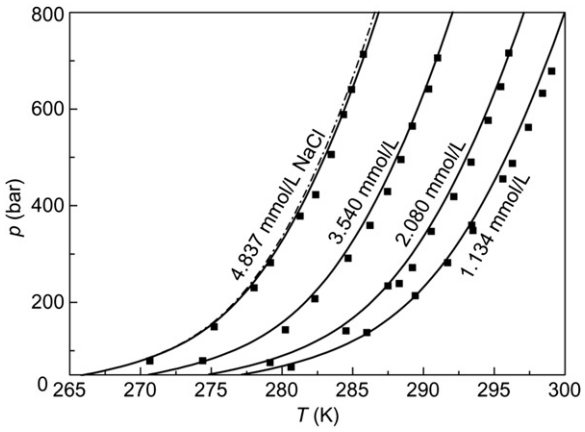

Figure 6 Prediction of the phase boundaries of CH_4 hydrate in CH_4–H_2O–NaCl system from the electrolyte parameters of Pitzer et al. (1984) for NaCl. The solid line represents the prediction by ignoring the effect of pressure on activity of water while the dashed line represents the prediction by including this effect.

2.3. Influence of porous medium

Methane hydrate of natural formation occurs within the pore spaces of sediments. Evidence shows that the pore sizes (Ruppel, 1997; Clennell et al., 1999), surface structure and mineral composition of the medium may influence the three-phase equilibrium conditions of gas hydrate. Recent workers have done many experiments to determine the three-phase equilibrium conditions of gas hydrate in porous medium (Handa and Stupin, 1992; Uchida et al., 1999, 2002; Seshadri et al., 2001; Seo et al., 2002; Smith et al., 2002a,b; Zhang et al., 2002; Seo and Lee, 2003; Anderson et al., 2003b; Aladko et al., 2004). These studies indicate that the capillary force can inhibit the formation of gas hydrate in small pores. However, the influence of the surface structure and the mineral composition of the medium on the formation of gas hydrate in previous studies are controversial. Recent experimental results of Riestenberg et al. (2003) and Uchida et al. (2004) show that they have minor influences on the methane hydrate equilibrium. Therefore, in this study, we will

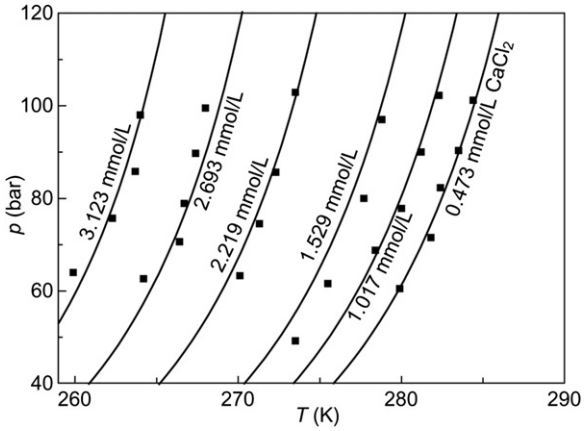

Figure 7 Prediction of the phase boundaries of CH_4 hydrate in the CH_4–H_2O–$CaCl_2$ system. The experimental data are from Kharrat and Dalmazzone (2003).

consider the factor of pore size and ignore factors of surface structure and mineral composition.

Based on the Gibbs–Thomas equation, Clennell et al. (1999) and Henry et al. (1999) proposed a formula that calculates the chemical difference of water caused by capillary forces. Some models (Clarke et al., 1999; Wilder et al., 2001; Klauda and Sandler, 2001, 2003; Seo et al., 2002) have referred to this formula. However, the formula is only suitable for chemical difference of water during the formation process. Subsequently, Dicharry et al. (2005) proposed a formula of the decomposition of hydrate in porous medium:

$$\Delta\mu_{\mathrm{w}}^{\mathrm{L}}(\mathrm{pore}) = \Delta\mu_{\mathrm{w}}^{\mathrm{L}}(\mathrm{bulk}) + V^{\beta}\frac{F\sigma_{HW}\cos\alpha}{r} \quad (15)$$

where V^{β} is the molar volume of water in the lattice of hydrate; F is the shape factor of the solid–liquid surface; α is the contact angle between solid and pore walls; r is the pore radius; σ_{HW} is the surface energy between the hydrate and liquid.

For Equation (15), we assume the following:

(1) The hydrate is in bulk state in the pores. Seo et al. (2002) found that the structure of CH_4 hydrate in silica gel pores (6.0 nm) is identical with those of bulk CH_4 hydrate through NMR spectroscopy;
(2) Liquid water is a continuous phase, because silica surface is hydrophilic and pores contain much more water than gas. In contrast, water on the pore walls is non-infiltrated with cos $\alpha = 1$. There is a layer of hydration (unfrozen water) (Handa and Stupin, 1992) whose thickness is 0.4 nm (Schreiber et al., 2001);
(3) There are boundaries between hydrate and water but no boundaries between hydrate and gas. Hydrate in pores is in contact with the continuous water phase. Because the surface energy between methane and liquid water is larger than that between hydrate and water, methane gas first fills the big pores forming the bulk phase. Therefore, we ignore the influence of capillary force on the chemical potential of methane in equilibrium in this study;
(4) The shape of pores and hydrate in pores is taken as cylindrical. Though there may be pores of complex shapes, the cylinder model fits well with the data of H–L–V equilibrium in synthetic porous medium and ice–liquid water equilibrium. Therefore, we think that cylinder model represents the shape of hydrate in pores of sediment substrate.

Strictly speaking, the r in Equation (15) denotes the radius of cylindrical hydrate and is equal to the pore radius minus the thickness of the hydration layer. The definition is the same in this study. In contrast, whereas previous models realized the presence of the hydrate layer, the r in these models is only the pore radius. F and σ_{HW} are quite important in Equation (15). Previous studies also have different choices on the values of these two parameters. The shape factor of boundaries is equal to 1 or 2 for cylindrical or spherical hydrate, respectively. Anderson et al. (2003b) and Llamedo et al. (2004) pointed out that the cylindrical shape corresponds to the decomposition state of hydrate and the spherical shape corresponds to the formation state of hydrate. For the delay of hydrate growth, the p–T condition for hydrate decomposition can represent the equilibrium condition more precisely. Therefore, we assume $F = 1$. However, most previous models mistakenly assume $F = 2$ and, thus, overestimate the inhibition effect of the capillary force on the H–L–V equilibrium.

There are no methods for measuring the surface energy of hydrate–liquid water up until now. Clennell et al. (1999) and Henry et al. (1999) postulated that the surface energy between hydrate and water (σ_{HW}) is equal to that between ice and water. Zhang et al. (2002) proved the above postulate through measuring H–L–V three-phase equilibrium in porous medium. The methods in a number of papers demonstrate that σ_{IW} is in the range of 25–33 mJ/m^3 (Hillig, 1998; Anderson et al., 2003a) at 273.15 K. The ice-water surface energy in this model comes from recent research (σ_{IW} 31.7 mJ/m^3) (Hillig, 1998), and this value is used to represent the hydrate–water surface energy. Uchida et al. (2002) calculated the methane hydrate–water surface energy based on hydrate equilibrium experimental data in porous medium. Nevertheless, they assumed the shape factor is 2 and got the result of (17 ± 3) mJ/m^3, about half of the ice–water surface energy. Anderson et al. (2003b) assumed the shape factor is 1 and got the result of (32 ± 2) mJ/m^3, which is in accord with the ice–water surface energy.

σ_{IW} may change with temperature, pore size (or curvature), or salinity of the solution changes. Tolman (1949) proposed the following equation that describes the influence of curvature on the surface energy:

$$\sigma = \sigma^{\infty}/\left(1+\frac{2\delta}{r}\right) \quad (16)$$

where σ^{∞} is the surface energy of plane interfaces and δ is the Tolman length, namely the interface thickness.

Bogdan (1997) thought the δ of ice–liquid water is 0.4186 nm at 273.15 K. The value is used in this study to calculate the influence of curvature on σ_{HW} ($\sigma_{HW}^{\infty} = 31.7$ mJ/m^3). For the process of hydrate decomposition, hydrate–water interface is cylindrical but because the curvature $2/r$ in Equation (16) refers to as spherical interface, we substitute $1/r$ for $2/r$.

Some research has shown that σ_{IW} decreases as the temperature decreases when it is lower than 273.15 K. However, we cannot determine whether the temperature-related parameters can extend to temperatures higher than 273.15 K or higher pressures. Jones (1973) and Hardy and Coriell (1973) measured the ice–NaCl surface energy, but their measurements had large uncertainties. Therefore, we ignored the σ_{HW} dependence on temperature and salinity.

3. Discussion

Sun and Duan (2005) and Duan and Sun (2006) built the model that accurately predicts the methane hydrate multi-phase equilibrium in water and in various electrolyte solutions. Fig. 8 is the comparison of this model's prediction with experimental data for methane hydrate three-phase equilibrium in seawater (Dholabhai et al., 1991; Dickens and Quinby-Hunt, 1994). The "seawater" in this study refers to standard seawater. Molality of major ions in 35 wt.‰ seawater is listed in Table 4, which is cited from Riley and Skirrow (1975) and Dickens and Quinby-Hunt (1997). The experimental pressure of methane hydrate H–L–V equilibrium in seawater is under 100×10^5 Pa, but we believe that our model can predict experiments with much higher pressures because our non-seawater model applies under pressures from 100×10^5 Pa as well as 2000×10^5 Pa.

Every curve in Fig. 9 represents p–T conditions when methane hydrate in pores of the same size reaches three-phase equilibrium. From the figure we know that the prediction of this model accords

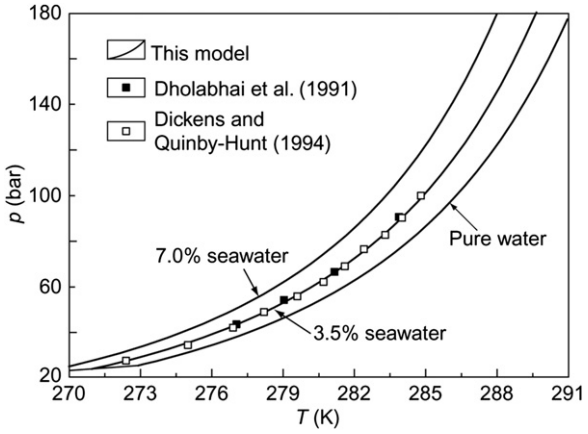

Figure 8 The prediction of this model for three-phase (H–L–V) equilibrium of methane hydrate in seawater.

with all of Anderson et al.'s (2003a) data, and most of the data of Uchida et al. (2002) and Seo et al. (2002). Because Uchida et al. (2002) and Seo et al. (2002) employed obviously different methods in measuring pores with diameter of 6.0 nm, their data differ. The prediction of dissociation pressures of methane hydrate in this present model is in accord with the former (Uchida et al., 2002), but a little larger than the latter (Seo et al., 2002).

In most cases, porous medium has no unified pore size, but the distribution of pore sizes has certain patterns. If the distribution pattern of pore sizes is introduced into this model without modifications of the model itself, this model still applies. The experimental data of Handa and Stupin (1992) and Smith et al. (2002a) show the constant volume $p-T$ conditions of hydrate dissociation in porous medium considering the pore size distribution. Their data are not compared with those of this model because of the absence of specific information on pore size distribution. The study of Dicharry et al. (2005) shows that the constant volume $p-T$ conditions of hydrate dissociation can be simulated by the Gibbs–Thomson equation and the known porous medium's cumulative volume.

Fig. 9 is the prediction of this model on methane hydrate three-phase equilibrium for different sizes of cylindrical pores. As Fig. 9 illustrates, the capillary force can inhibit the formation of methane hydrate. As pore size decreases, the dissociation temperature of methane hydrate also decreases. The inhibitory effect of cylindrical pores with diameter of 32 nm is the same as that of standard seawater in 283 K.

Table 4 The molality (mol/kg H_2O) of major ions in 35 wt.‰ seawater, in 30 wt.‰ oxic seawater and 30 wt.‰ euxinic seawater.

Ion type	35 wt.‰ seawater[a]	30 wt.‰ oxic seawater[b]	30 wt.‰ euxinic seawater[b]
Na^+	0.48559	0.41596	0.44847
K^+	0.01058	0.00880	0.00768
Ca^+	0.01065	0.00918	0.00606
Mg^+	0.05517	0.04732	0.02808
Cl^-	0.56541	0.48492	0.51210
SO_4^{2-}	0.02926	0.02507	0
HCO_3^-	0.00241	0.00207	0.01515
Br^-	0.00087	0.00073	0.00323
NH_4^+	0	0	0.00606

[a] Riley and Skirrow (1975).
[b] Dickens and Quinby-Hunt (1997).

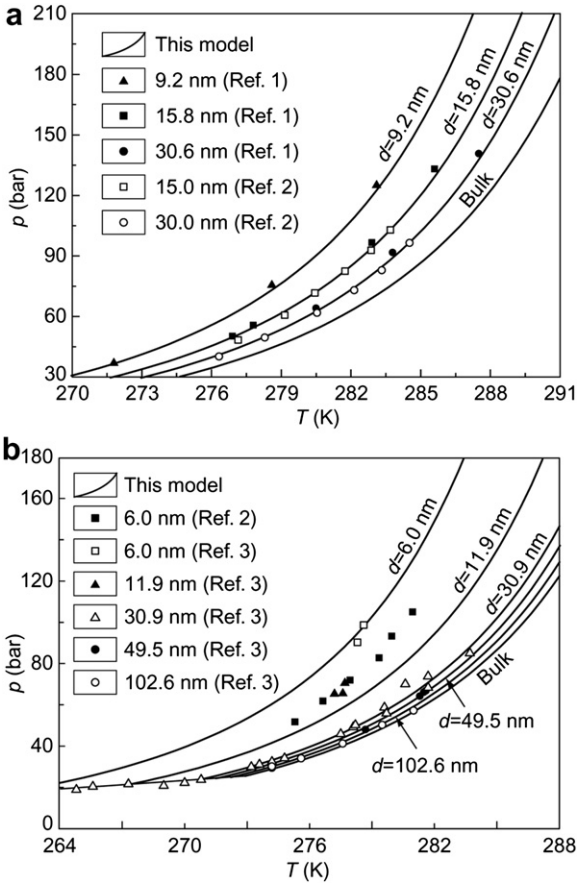

Figure 9 The prediction of capillary force on H–L–V equilibrium of methane hydrate in the CH_4–H_2O system. The experimental data are from Ref. 1: Anderson et al. (2003a), Ref. 2: Seo et al. (2002), Ref. 3: Uchida et al. (2002).

4. Conclusion

In considering the influence of temperature, pressure, salinity and capillary force on the hydrate equilibrium, this paper presents an accurate thermodynamic model in predicting the methane hydrate stability in seawater. The model employs van der Waals and Platteeuw (1959) hydrate model and the angle-dependent *ab initio* intermolecular potentials to calculate the chemical potential of hydrate. The influence of capillary force in porous media on the H–L–V equilibrium can be determined by the Gibbs–Thomson equation into which the correct hydrate–water contact parameters are substituted. According to the latest research, the influences of medium surface structure and mineral composition on equilibrium conditions of gas hydrate are very small, so they are ignored in this study. The Pitzer model is used in this model where the calculation of water and methane activity coefficient is involved in the methane–seawater system.

By comparing the model predictions and experimental data, we can see that our model can accurately predict the multi-phase equilibrium conditions of methane hydrate in seawater and porous media. Salt dissolved in seawater and the capillary force in small

pores will increase the pressure required for the formation of methane hydrate under certain temperatures.

References

Aasberg-Petersen, K., Stenby, E., Fredenslund, A., 1991. Predictions of high-pressure gas solubilities in aqueous mixtures of electrolytes. Industrial and Engineering Chemistry Research 30, 2180−2185.

Aladko, E.Y., Dyadin, Y.A., Fenelonov, V.B., Larionov, E.G., Mel'gunov, M.S., Manakov, A.Y., Nesterov, A.N., Zhurko, F.V., 2004. Dissociation conditions of methane hydrate in mesoporous silica gels in wide ranges of pressure and water content. Journal of Physical Chemistry B108, 16540−16547.

Anderson, B.J., Llamedo, M., Tohidi, B., Burgass, R.W., 2003a. Experimental measurement of methane and carbon dioxide clathrate hydrate equilibria in mesoporous silica. Journal of Physical Chemistry B107, 3507−3514.

Anderson, R., Llamedo, M., Tohidi, B., Burgass, R.W., 2003b. Characteristics of clathrate hydrate equilibria in mesopores and interpretation of experimental data. Journal of Physical Chemistry B107, 3500−3506.

Anderson, B.J., Tester, J.W., Trout, B.L., 2004. Accurate potentials for argon−water and methane−water interactions via *ab initio* methods and their application to clathrate hydrates. Journal of Physical Chemistry B108, 18705−18715.

Ballard, A.L., Sloan, E.D., 2002. The next generation of hydrate prediction: I. Hydrate standard states and incorporation of spectroscopy. Fluid Phase Equilibria 194−197, 371−383.

Bogdan, A., 1997. Thermodynamics of the curvature effect on ice surface tension and nucleation theory. Journal of Chemical Physics 106, 1921−1929.

Bolis, G., Clementi, E., Wertz, D.H., Scheraga, H.A., Tosi, C., 1983. Interaction of methane and methanol with water. Journal of American Chemistry Society 105, 355−360.

Cao, Z.T., Tester, J.W., Trout, B.L., 2001. Computation of the methane−water potential energy hypersurface via *ab initio* methods. Journal of Chemical Physics 115, 2550−2559.

Chen, C.C., Evans, L.B., 1986. A local composition model for the excess Gibbs energy of aqueous electrolyte systems. American Institute of Chemical Engineers Journal 32, 444−454.

Chen, G.J., Guo, T.M., 1998. A new approach to gas hydrate modeling. Chemical Engineering Journal 71, 145−151.

Chueh, P.L., Prausnitz, J.M., 1967. Vapor−liquid equilibria at high pressures. Vapor-phase fugacity coefficients in nonpolar and quantum−gas mixtures. Industrial and Engineering Chemistry Fundamentals 6, 492−498.

Clarke, M.A., Pooladi-Darvish, M., Bishnoi, P.R., 1999. A method to predict equilibrium conditions of gas hydrate formation in porous media. Industrial and Engineering Chemistry Research 38, 2485−2490.

Clennell, M.B., Hovland, M., Booth, J.S., Henry, P., Winters, W.J., 1999. Formation of natural gas hydrates in marine sediments: I. Conceptual model of gas hydrate growth conditioned by host sediment properties. Journal of Geophysical Research Solid Earth 104 (B10), 22985−23003.

De Roo, J.L., Peters, C.J., Lichtenthaler, R.N., Diepen, M., 1983. Occurrence of methane hydrate in saturated and unsaturated solutions of sodium chloride and water in dependence of temperature and pressure. American Institute of Chemical Engineers Journal 29, 651−657.

Dholabhai, P.D., Englezos, P., Kalogerakis, N., Bishnoi, P.R., 1991. Equilibrium conditions for methane hydrate formation in aqueous mixed electrolyte solutions. The Canadian Journal of Chemical Engineering 69 (3), 800−805.

Dicharry, C., Gayet, P., Marion, G., Graciaa, A., Nesterov, A.N., 2005. Modeling heating curve for gas hydrate dissociation in porous media. Journal of Physical Chemistry B109, 17205−17211.

Dickens, G.R., 2003. Rethinking the global carbon cycle with a large, dynamic and microbially mediated gas hydrate capacitor. Earth and Planetary Science Letters 213, 169−183.

Dickens, G.R., Quinby-Hunt, M.S., 1994. Methane hydrate stability in seawater. Geophysical Research Letters 21, 2115−2118.

Dickens, G.R., Quinby-Hunt, M.S., 1997. Methane hydrate stability in pore water: a simple theoretical approach for geophysical applications. Journal of Geophysical Research 102 (B1), 773−783.

Duan, Z.H., Mao, S.D., 2006. A thermodynamic model for calculating methane solubility, density and gas phase composition of methane bearing aqueous fluids from 273 to 523 K and from 1 to 2000 bar. Geochimica et Cosmochimica Acta 70, 3369−3386.

Duan, Z.H., Moller, N., Weare, J.H., 1992a. The prediction of methane solubility in natural waters to high ionic strength from 0 to 250 °C and from 0 to 1600 bar. Geochimica et Cosmochimica Acta 56, 1451−1460.

Duan, Z.H., Moller, N., Weare, J.H., 1992b. An equation of state for the CH_4−CO_2−H_2O system: I. Pure systems from 0 to 1000 °C and 0 to 8000 bar. Geochimica et Cosmochimica Acta 56, 2605−2617.

Duan, Z.H., Sun, R., 2003. An improved model calculating CO_2 solubility in pure water and aqueous NaCl solutions from 273 to 533 K and from 0 to 2000 bar. Chemical Geology 193, 257−271.

Duan, Z.H., Sun, R., 2006. A model to predict phase equilibrium of CH_4 and CO_2 clathrate hydrate in aqueous electrolyte solutions. American Mineralogist 91, 1346−1354.

Dubessy, J., Thiery, R., Canals, M., 1992. Modeling of phase equilibria involving mixed gas clathrates: application to the determination of molar volume of the vapour phase and salinity of the aqueous solution in fluid inclusions. European Journal of Mineralogy 4, 873−884.

Englezos, P., Bishnoi, P.R., 1988. Prediction of gas hydrate formation conditions in aqueous electrolyte solutions. American Institute of Chemical Engineers Journal 34, 1718−1721.

Felmy, A.R., Weare, J.H., 1986. The prediction of borate mineral equilibria in natural waters: application to Searles Lake, California. Geochimica et Cosmochimica Acta 50, 2771−2783.

Greenberg, J.P., Moller, N., 1989. The prediction of mineral solubilities in natural waters: a chemical equilibrium model for the Na−K−Mg−Cl−SO_4−H_2O system to high concentration from 0 to 250 °C. Geochimica et Cosmochimica Acta 53, 2503−2518.

Handa, Y.P., Stupin, D., 1992. Thermodynamic properties and dissociation characteristics of methane and propane hydrates in 70A-Radius silica gel pores. Journal of Physical Chemistry 96, 8599−8603.

Hardy, S.C., Coriell, S.R., 1973. Surface tension and interface kinetics of ice crystals freezing and melting in sodium chloride solutions. Journal of Crystal Growth 20, 292−300.

Harvie, C.E., Moller, N., Weare, J.H., 1984. The prediction of mineral solubilities in natural waters: the Na−K−Mg−Ca−H−Cl−SO_4−OH−HCO_3−CO_3−CO_2−H_2O system to high ionic strengths at 25 °C. Geochimica et Cosmochimica Acta 48, 723−751.

Henry, P., Thomas, M., Clennell, M.B., 1999. Formation of natural gas hydrates in marine sediments 2. Thermodynamic calculations of stability conditions in porous sediments. Journal of Geophysical Research Solid Earth 104 (B10), 23005−23022.

Hillig, W.B., 1998. Measurement of interfacial free energy for ice/water system. Journal of Crystal Growth 183, 463−468.

Holder, G.D., Corbin, G., Papadopoulos, K.D., 1980. Thermodynamic and molecular properties of gas hydrates from mixtures containing methane, argon and krypton. Industrial and Engineering Chemistry Fundamentals 19, 282−286.

Jager, M.D., Sloan, E.D., 2001. The effect of pressure on methane hydration in pure water and sodium chloride solutions. Fluid Phase Equilibria 185, 89−99.

Jhaveri, J., Robinson, D.B., 1965. Hydrates in the methane−nitrogen system. The Canadian Journal of Chemical Engineering 43, 75−78.

Jones, D.R.H., 1973. The measurement of solid−liquid interfacial energies from the shapes of grain-boundary grooves. Philosophical Magazine 27, 569−584.

Jorgensen, W.J., Chandrasekhar, J., Madura, J.D., Impey, R.W., Klein, M.L., 1983. Comparison of simple potential functions for simulating liquid water. Journal of Chemical Physics 79, 926−935.

Kharrat, M., Dalmazzone, D., 2003. Experimental determination of stability conditions of methane hydrate in aqueous calcium chloride solutions using high pressure differential scanning calorimetry. Journal of Chemical Thermodynamics 35, 1489−1505.

Klauda, J.B., Sandler, S.I., 2001. Modeling gas hydrate phase equilibria in laboratory and natural porous media. Industrial and Engineering Chemistry Research 40, 4197−4208.

Klauda, J.B., Sandler, S.I., 2002. *Ab initio* intermolecular potentials for gas hydrates and their predictions. Journal of Physical Chemistry B106, 5722−5732.

Klauda, J.B., Sandler, S.I., 2003. Predictions of gas hydrate phase equilibria and amounts in natural sediment porous media. Marine and Petroleum Geology 20, 459−470.

Kobayashi, R., Katz, D.L., 1949. Methane hydrate at high pressure. Journal of Petroleum Technology 1, 66−70.

Latajka, S., Scheiner, S., 1987. Basis sets for molecular interactions. 2. Application to H_3N−HF, H_3N−HOH, H_2O−HF, $(NH_3)_2$ and H_3CH−OH_2. Journal of Computational Chemistry 8, 674−682.

Lee, S.Y., Holder, G.D., 2002. Model for gas hydrate equilibria using a variable reference chemical potential: part 1. American Institute of Chemical Engineers Journal 48, 161−167.

Llamedo, M., Anderson, R., Tohidi, B., 2004. Thermodynamic prediction of clathrate hydrate dissociation conditions in mesoporous media. American Mineralogist 89, 1264−1270.

Lunine, J.I., Stevenson, D.J., 1987. Clathrate and ammonia hydrates at high-pressure: application to the origin of methane on titan. Icarus 70, 61−77.

Maekawa, T., 2001. Equilibrium conditions for gas hydrates of methane and ethane mixtures in pure water and sodium chloride solution. Geochemical Journal 35, 59−66.

Marshall, D.R., Saito, S., Kobayashi, R., 1964. Hydrates at high pressures. Methane−water and argon−water systems. American Institute of Chemical Engineers Journal 10, 202−205.

McLeod, H.O., Campbell, J.M., 1961. Natural gas hydrates at pressures to 10 000 psia. Journal of Petroleum Technology 13, 590−594.

Moller, N., 1988. The prediction of mineral solubilities in natural waters: a chemical equilibrium model for the Na−Ca−Cl−SO_4−H_2O system, to high temperature and concentration. Geochimica et Cosmochimica Acta 52, 821−837.

Monnin, C., 1990. The influence of pressure on the activity coefficients of the solutes and the solubility of minerals in the system Na−Ca−Cl−SO_4−H_2O to 200 °C and 1 kbar, and to high NaCl concentration. Geochimica et Cosmochimica Acta 54, 3265−3282.

Nakano, S., Moritoki, M., Ohgaki, K., 1999. High-pressure phase equilibrium and Raman microprobe spectroscopic studies on the methane hydrate system. Journal of Chemical Engineering Data 44, 254−257.

Ng, H.J., Robinson, D.B., 1976. The measurement and prediction of hydrate formation in liquid hydrocarbon−water systems. Industrial and Engineering Chemistry Fundamentals 15, 293−298.

Novoa, J.J., Tarron, B., Whangbo, M.H., Williams, J.N., 1991. Interaction energies associated with short intermolecular contacts of C−H bonds. *Ab initio* computational study of the C−H…O contact interaction in CH_4…OH_2. Journal of Chemical Physics 95, 5179−5186.

Pabalan, R.T., Pitzer, K.S., 1987. Thermodynamics of concentrated electrolyte mixtures and the prediction of mineral solubilities to high temperatures for mixtures in the system Na−K−Mg−Cl−SO_4−OH−H_2O. Geochimica et Cosmochimica Acta 51, 2429−2443.

Parrish, W.R., Prausnitz, J.M., 1972. Dissociation pressures of gas hydrates formed by gas mixtures. Industrial and Engineering Chemistry Process Design Development 11, 26−35.

Peng, D.Y., Robinson, D.B., 1976. A new two-constant equation of state. Industrial and Engineering Chemistry Fundamentals 15, 59−64.

Pitzer, K.S., 1975. Thermodynamics of electrolytes. V. Effects of higher-order electrostatic terms. Journal of Solution Chemistry 4, 249−265.

Pitzer, K.S., 1991. Theory and data correlation. In: Pitzer, K.S. (Ed.), Activity Coefficients in Electrolyte Solutions. CRC Press, London, pp. 75−153.

Pitzer, K.S., Kim, J., 1974. Thermodynamics of electrolytes. IV. Activity and osmotic coefficients for mixed electrolytes. Journal of the American Chemical Society 96, 5701−5707.

Pitzer, K.S., Mayorga, G., 1973. Thermodynamics of electrolytes. II. Activity and osmotic coefficients for strong electrolytes with one or both ions univalent. Journal of Physical Chemistry 77, 2300−2308.

Pitzer, K.S., Mayorga, G., 1974. Thermodynamics of electrolytes. III. Activity and osmotic coefficients for 2−2 electrolytes. Journal of Solution Chemistry 3, 539−546.

Pitzer, K.S., Peiper, J.C., Busey, R.H., 1984. Thermodynamic properties of aqueous sodium chloride solutions. Journal of Physical and Chemical Reference Data 13, 1−102.

Pitzer, K.S., Silvester, L.F., 1976. Thermodynamics of electrolytes. VI. Weak electrolytes including H_3PO_4. Journal of Solution Chemistry 5, 269−277.

Riestenberg, D., West, O., Lee, S., McCallum, S., Phelps, T.J., 2003. Sediment surface effects on methane hydrate formation and dissociation. Marine Geology 198, 181−190.

Riley, J.P., Skirrow, G., 1975. Chemical Oceanography. Academic Press Inc, New York. 59−72.

Ruppel, C., 1997. Anomalously cold temperatures observed at the base of the gas hydrate stability zone on the U. S. Atlantic passive margin. Geology 25, 699−702.

Schreiber, A., Ketelsen, I., Findenegg, G.H., 2001. Melting and freezing of water in ordered mesoporous silica materials. Physical Chemistry Chemical Physics 3, 1185−1195.

Seo, Y., Lee, H., 2003. Hydrate phase equilibria of the ternary CH_4 + NaCl + water, CO_2 + NaCl + water and CH_4 + CO_2 + water mixtures in silica gel pores. Journal of Physical Chemistry B107, 889−894.

Seo, Y., Lee, H., Uchida, T., 2002. Methane and carbon dioxide hydrate phase behavior in small porous silica gels: three-phase equilibrium determination and thermodynamic modeling. Langmuir 18, 9164−9170.

Seshadri, K., Wilder, J.W., Smith, D.H., 2001. Measurements of equilibrium pressures and temperatures for propane hydrate in silica gels with different pore-size distributions. Journal of Physical Chemistry B105, 2627−2631.

Setzmann, U., Wagner, W., 1991. A new equation of state and tables of thermodynamic properties for methane covering the range from the melting line to 625 K at pressures up to 1000 MPa. Journal of Physical and Chemical Reference Data 20, 1061−1151.

Sloan, E.D., 1998. Clathrate Hydrates of Natural Gases. Marcel Decker, New York, pp. 56—71.

Smith, D.H., Wilder, J.W., Seshadri, K., 2002a. Methane hydrate equilibria in silica gels with broad pore-size distributions. AIChE Journal 48, 393−400.

Smith, D.H., Wilder, J.W., Seshadri, K., 2002b. Thermodynamics of carbon dioxide hydrate formation in media with broad pore-size distributions. Environmental Science and Technology 36, 5192−5198.

Soave, G., 1972. Equilibrium constants from a modified Redlich−Kwong equation of state. Chemical Engineering Science 27, 1197−1203.

Spencer, R.J., Moller, N., Weare, J.H., 1990. The prediction of mineral solubilities in natural waters: a chemical equilibrium model for the Na−K−Ca−Mg−Cl−SO_4−H_2O system at temperatures below 25 °C. Geochimica et Cosmochimica Acta 54, 575−590.

Sun, R., Duan, Z.H., 2005. Prediction of CH_4 and CO_2 hydrate phase equilibrium and cage occupancy from *ab initio* intermolecular potentials. Geochimica et Cosmochimica Acta 69, 4411−4424.

Sun, R., Huang, Z., Duan, Z.H., 2003. A new equation of state and Fortran 77 program to calculate vapor−liquid phase equilibria of CH_4−H_2O system at low temperature. Computational Geosciences 29, 1291−1299.

Szczesniak, M.M., Chalasinski, G., Cybulski, S.M., Cieplak, P., 1993. *Ab initio* study of the potential energy surface of CH_4−H_2O. Journal of Chemical Physics 98, 3078−3089.

Tee, L.S., Gotoh, S., Stewart, W.E., 1966. Molecular parameters for normal fluids: the Kihara potential with spherical core. Industrial and Engineering Chemistry Fundamentals 5, 363−367.

Tohidi, B., Danesh, A., Todd, A.C., 1995. Modeling single and mixed electrolyte solutions and its applications to gas hydrates. Chemical Engineering Research and Design 73 (A), 464−472.

Tolman, R.C., 1949. The effect of droplet size on surface tension. Journal of Chemical Physics 17, 333−337.

Uchida, T., Ebinuma, T., Ishizaki, T., 1999. Dissociation condition measurements of methane hydrate in confined small pores of porous glass. Journal of Physical Chemistry B103, 3659−3662.

Uchida, T., Ebinuma, T., Takeya, S., Nagao, J., Narita, H., 2002. Effects of pore sizes on dissociation temperatures and pressures of methane, carbon dioxide and propane hydrates in porous media. Journal of Physical Chemistry B106, 820−826.

Uchida, T., Takeya, S., Chuvilin, E.M., Ohmura, R., Nagao, J., Yakushev, V.S., Istomin, V.A., Minagawa, H., Ebinuma, T., Narita, H., 2004. Decomposition of methane hydrates in sand, sandstone, clays and glass beads. Journal of Geophysical Research Solid Earth 109, B05206.

van der Waals, J.H., Platteeuw, J.C., 1959. Clathrate solutions. In: Prigogine, I. (Ed.), Advances in Chemical Physics. Interscience, New York, pp. 1−57.

Verma, V.K., 1974. Gas Hydrates from Liquid Hydrocarbon−Water Systems. University of Michigan, Michigan.

Wilder, J.W., Seshadri, K., Smith, D.H., 2001. Modeling hydrate formation in media with broad pore size distributions. Langmuir 17, 6729−6735.

Xu, W., Germanovich, L.N., 2006. Excess pore pressure resulting from methane hydrate dissociation in marine sediments: a theoretical approach. Journal of Geophysical Research Solid Earth 111, B01104.

Yang, S.O., Cho, S.H., Lee, H., Lee, C.S., 2001. Measurement and prediction of phase equilibria for water + methane in hydrate forming conditions. Fluid Phase Equilibria 185, 53−63.

Zatsepina, O.Y., Buffett, B.A., 1998. Thermodynamic conditions for the stability of gas hydrate in the seafloor. Journal of Geophysical Research 103, 24127−24139.

Zhang, W., Wilder, J.W., Smith, D.H., 2002. Interpretation of ethane hydrate equilibrium data for porous media involving hydrate−ice equilibria. AIChE Journal 48, 2324−2331.

Zuo, Y.X., Guo, T.M., 1991. Extension of the Patel−Teja equation of state to the prediction of the solubility of natural gas in formation water. Chemical Engineering Science 46, 3251−3258.